Bull. Chem. Soc. Jpn., 71, 1817—1823 (1998)

IR Sensing of the Electronic Structure in the Mixed-Valence States of Iron Carbonyl-Attached Biferrocene and Terferrocene

Takashi Hirao, Kunitsugu Aramaki, and Hiroshi Nishihara[*,†]

Department of Chemistry, Faculty of Science and Technology, Keio University, Hiyoshi, Yokohama 223-0061

†Department of Chemistry, School of Science, The University of Tokyo, Hongo, Tokyo 113-0033

(Received January 19, 1998)

Ferrocene, 1,1,″-biferrocene and 1,1″ : 1‴,1⁗-terferrocene derivatives involving a (cycopentadiene)$Fe(CO)_3$ moiety were synthesized; the ν(CO) peak frequency shifts during their redox processes were monitored by the IRAS technique. All the complexes give two ν(CO) peaks, which shift to higher wavenumbers (12—18 cm^{-1}) by the oxidation from the most reduced (all Fe's are Fe(II)) to the most oxidized (all Fe's are Fe(III)) forms. The biferrocene derivative in the monocationic form gives peaks at wavenumbers between those for neutral and dicationic forms, probably because the rate of electron-transfer affording two electronic isomers, Red–Ox–[FeCO] and Ox–Red–[FeCO], where Red, Ox, and [FeCO] refer to reduced and oxidized forms of a ferrocene unit, and a [(η^4-cyclopentadiene)$Fe(CO)_3$] moiety, respectively, is slower than or comparable to the time scale of IR (10^{11}—10^{12} s^{-1}). The terferrocene derivative shows ν(CO) frequency changes corresponding to the three-step $1e^-$ oxidation processes. The shift is most significant in the second oxidation step, implying that the largest change in charge is that of the ferrocene unit nearest to $Fe(CO)_3$. This is in principle consistent with the elucidation of the oxidation process via thermodynamically favorable electronic isomers based on the interaction energy between neighboring oxidized and reduced sites:

Red–Red–Red–[FeCO] ⟶ Red–Ox–Red–[FeCO] ⟶ Ox–Red–Ox–[FeCO] ⟶ Ox–Ox–Ox–[FeCO].

Polymers with a linear sequence of cooperating redox centers are of great interest in view of providing electronically and magnetically functional materials.[1] Oligo(1,1′-ferrocenylene) can be a model of such linear redox combination with inter-nuclei electronic communication,[2] but the unsubstituted one loses considerable solubility with the increase in the number of nuclei. Their electrochemistry has been investigated up to the tetramer and a low molecular-weight polymer.[3,4]

We have recently synthesized soluble oligoferrocenylene derivatives, **1a**—**5a** and **1b**—**7b**,[5,6] (Scheme 1) that can be used for the analysis of redox potential dependencies on the number of nuclei using a theory based on the neighboring site interaction energy between oxidized (Ox) and reduced (Red) sites, u_{OR}, that between Ox and Ox, u_{OO}, and that between Red and Red, u_{RR}, demonstrated by Aoki and Chen.[7] In this theory, the oligomer is assumed to be a sequence of Red and Ox and the thermodynamically most favorable electronic isomers in the mixed valence states are determined mainly by the total u_{OR} value. For example, a redox trimer

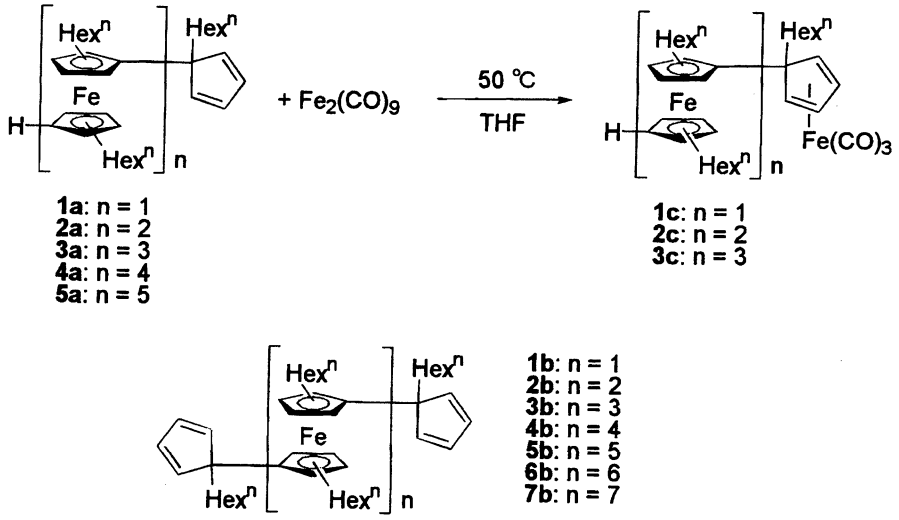

Scheme 1.

gives two possible electronic isomers in its two mixed valence states, and the theory indicates that Red–Ox–Red is thermodynamically more favorable than Ox–Red–Red, and also Ox–Red–Ox is more favorable than Ox–Ox–Red.

Analysis for the redox potentials of oligo(dihexylferrocenylene) has proved that their dependencies on the number of nuclei can not be interpreted with only the neighboring site interaction energies, while addition of the second neighboring site interaction energy, u_{OXR} reproduces the experimental results.[6,8] However, the magnitude of u_{OXR}, is small, -3.8 kJ mol^{-1} and about one-forth of u_{OR},[9] suggesting that the positive charge in the molecule is considerably localized on the "Ox" sites. This is in accordance with our primary assumption that each oxidation state of the oligomer can be expressed as a combination of Red and Ox.

Electron delocalization between Red and Ox for monocation of 1,1″-biferrocene and its derivatives has been investigated using several methods such as near-IR, IR, far-IR, Mössbauer and ESR spectroscopy in addition to the elecrochemical measurements.[2,3,10–21] As for infrared spectroscopy, the bands of perpendicular C–H bending mode show the oxidation state of ferrocene units.[18–23] The analysis of this band is a powerful tool to examine the electron-transfer rate against the IR time scale, but cannot inform about the electronic structure of the favorable electronic isomers in the mixed valence states of 1,1″ : 1‴,1⁗-terferrocene as noted above.

In the present study we synthesized forrocene, biferrocene and terferrocene derivatives, **1c—3c**, involving an iron tricarbonyl moiety which senses the oxidation state of the ferrocene unit attached to the (cyclopentadiene)Fe(CO)$_3$ moiety ([FeCO]) and we carried out the measurements of infrared refraction absorption spectroscopy (IRAS) while controlling the oxidation state of the molecule electrochemically. Reversible wavenumber shifts of ν(CO) by changing the redox state are clearly observed. The degree of the shifts thus obtained for **2c** and **3c** is discussed with the electronic structure and charge balance among redox units in the mixed-valenece state(s).

Experimental

Ferrocenes, **1a**, **2a**, and **3a** were prepared as reported previously.[5] Iron enneacarbonyl was prepared from Fe(CO)$_5$ (Aldrich) according to the method in the literature.[24] Anhydrous solvents were obtained from Kanto Chemicals. Tetrabutylammonium perchlorate was obtained from Tomiyama Chemicals as lithium battery grade. Dichloromethane used for electrochemical measurements was a HPLC grade chemical from Kanto Chemicals. Infrared and ^{1}H NMR spectra were recorded with Shimadzu FT-IR 8100M and JEOL GX400 spectrometers, respectively. IRAS measurements combined with an electrochemical setup were carried out with a Bio-Rad FTS-454RD spectrometer, a Toho Technical Research 2020 potentio/galvanostat and a 2230 function generator.

Preparation of [(η^5-C$_5$H$_4$Hex^n)Fe{η^5-C$_5$H$_3$Hex^n-(η^4-C$_5$H$_4$Hex^n)Fe(CO)$_3$}] (1c). All the manipulations were carried out under nitrogen or argon except when otherwise stated. A mixture of **1a** (115 mg, 0.23 mmol) and Fe$_2$(CO)$_9$ (209 mg, 0.58 mmol) in 10 dm^3 THF was stirred at 50 °C for 1 h. The solution was filtered through a 0.45 μm membrane filter, and the filtrate was dried under vacuum. The rsidue was dissolved in toluene and separated with a JAI LC908 recycling HPLC apparatus equipped with JAIGEL 2H and 3H columns to give a yellow component. This component was separated by TLC (Merck silica gel 60F$_{254}$ plates) with hexane–chloroform (10 : 1) as an eluent into two components with R_f = 0.65 and 0.48. The former were found to be **1a** and the objective compound **1c** was obtained from the latter component as yellow oil: Yield 20 mg, 14%. Found: C, 67.48; H, 7.84%. Calcd for C$_{36}$H$_{50}$Fe$_2$O$_3$: C, 67.30; H, 7.84%. IR (KBr) 2039, 1965 cm^{-1} (ν_{CO}); ^{1}H NMR (CDCl$_3$) δ = 5.43 (2H, m, CH of η^4-hexylcyclopentadiene moiety), 4.1—3.7 (7H, m, CH of η^5-hexylcyclopentadienyl moieties), 3.07 (2H, m, CH of η^4-hexylcyclopentadienyl moiety), 2.4—2.0 (6H, m, terminal CH$_2$ of hexyl moieties), 1.6—1.0 (24H, m, CH$_2$ of hexyl moieties), 1.0—0.8 (9H, m, C*H*$_3$).

Preparation of [(η^5-C$_5$H$_4$Hex^n)Fe(η^5-C$_5$H$_3$Hex^n-η^5-C$_5$H$_3$Hex^n)Fe{η^5-C$_5$H$_3$Hex^n-(η^4-C$_5$H$_4$Hex^n)Fe(CO)$_3$}] (2c) and [(η^5-C$_5$H$_4$Hex^n)Fe(η^5-C$_5$H$_3$Hex^n-η^5-C$_5$H$_3$Hex^n)Fe(η^5-C$_5$H$_3$Hex^n-η^5-C$_5$H$_3$Hex^n)Fe{η^5-C$_5$H$_3$Hex^n-(η^4-C$_5$H$_4$Hex^n)Fe(CO)$_3$}] (3c). Biferrocene and terferrocene derivatives **2c** and **3c** were prepared from **2a** and **3a**, respectively, in a manner similar to that described for **1c**. Their isolation by TLC was, however, incomplete because of the R_f values for Fe(CO)$_3$-free and attached forms were very close, so that sample were obtained as mixtures of **2a**+**2c** with the mole ratio of **2a**/**2c** = 0.5 and **3a**+**3c** with the mole ratio of **3a**/**3c** = 1.1.

2a+2c: IR (KBr) 2038, 1965 cm^{-1} (ν_{CO}); ^{1}H NMR (CDCl$_3$) δ = 6.3 (1.3H, m, CH of end hexylcyclopentadiene moiety of **2a**), 5.3—5.4 (1.3H, m, CH of η^4-hexylcyclopentadiene moiety of **2c**), 4.2—3.5 (13H, m, CH of η^5-hexylcyclopentadienyl moieties), 3.04 (1.3H, m, CH of η^4-hexylcyclopentadienyl moiety of **2c**), 2.4—2.0 (10H, m, terminal CH$_2$ of hexyl moieties), 1.6—1.0 (40H, m, CH$_2$ of hexyl moieties), 1.0—0.8 (15H, m, CH$_3$).

3a+3c: IR (KBr) 2038, 1964 cm^{-1} (ν_{CO}); ^{1}H NMR (CDCl$_3$) δ = 6.3 (2.1H, m, CH of end hexylcyclopentadiene moiety of **3a**), 5.3—5.4 (1.0H, m, CH of η^4-hexylcyclopentadiene moiety of **3c**), 4.1—3.6 (19H, m, CH of η^5-hexylcyclopentadienyl moieties), 3.02 (1.0H, m, CH of η^4-hexylcyclopentadienyl moiety of **3c**), 2.4—2.0 (14H, m, terminal CH$_2$ of hexyl moieties), 1.6—1.0 (56H, m, CH$_2$ of hexyl moieties), 1.0—0.8 (21H, m, CH$_3$).

Cyclic Voltammetry. A glassy carbon (GC) rod (Tokai Carbon GC-20, diameter: 5 mm) was embedded in Pyrex glass and the cross section was used as a working electrode. Cyclic voltammetry was carried out in a standard one-compartment cell equipped with a Pt wire counter electrode and an Ag/Ag$^+$ (10 mmol dm^{-3} AgClO$_4$ in 0.1 mol dm^{-3} *n*-Bu$_4$NClO$_4$–MeCN, $E^{0\prime}$ (ferrocenium/ferrocene) = 0.21 V vs. Ag/Ag$^+$) reference electrode with a BAS CV-50W voltammetric analyzer.

IR-Spectroelectrochemistry. The electrochemical cell for IRAS measurements was similar to that reported previously by Ito and his coworkers.[25] It was equipped with a Pt disk working electrode, a Pt wire counter electrode and a Ag/Ag$^+$ reference electrode. An IR spectrum first measured in a deaerated 0.1 mol dm^{-3} *n*-Bu$_4$NClO$_4$–CH$_2$Cl$_2$ solution was defined as the background spectrum; then a sample was added to the solution and cyclic voltammetry was carried out. IR spectra of the sample in a given oxidation state were measured after the potential was applied and the current decreased to the background level.

Results and Discussion

Synthesis and Redox Properties. Iron carbonyl complexes of ferrocenes, **1c—3c**, were synthesized by a re-

action of free cyclopentadiene moieties in **1a**—**3a**, with $Fe_2(CO)_9$ (Scheme 1), a regular method to prepare (η^4-cyclopentadiene)$Fe(CO)_3$.[26] The ferrocene monomer **1c** was isolated using silica gel column chromatography, but the dimer, **2c** and the trimer, **3c** could not be separated from iron carbonyl-free ferrocenes, **2a** and **3a**, respectively, because of the very close R_f values. The mol ratios of **2a**/**2c** and **3a**/**3c** used in this study were determined to be 0.5 and 1.1, respectively, from their ^{1}H NMR spectra, where δ values for protons on the cyclopentadiene moiety shifts from 6.3 to 5.4—5.3 and 2.4—2.0 by coordinating to iron. Fortunately, the contamination of iron carbonyl-free ferrocenes in **2c** and **3c** does not give any disadvantageous effect on interpreting the results of the IR-spectroelectrochemical study as described below (Scheme 2). Infrared spectra of **1c**—**3c** show two ν(CO) absorption peaks typical to (η^4-diene)$Fe(CO)_3$ complexes: One is strong and sharp at ca. 2040 cm^{-1} (A′(1)) and the other is medium and broad at ca. 1965 cm^{-1} (A′(2) and A″).[27,28]

Cyclic voltammograms of **1c**, **2a**+**2c**, and **3a**+**3c** in 0.1 mol dm^{-3} n-Bu_4NClO_4–CH_2Cl_2 are given in Fig. 1. Oxidation of the ferrocene moiety in **1c** occurs at $E^{0\prime} = 0.04$ V vs. Ag/Ag^+, similar to that for **1a** ($E^{0\prime} = 0.04$ V),[5] indicating that the bonding to (cyclopentadiene)$Fe(CO)_3$ does not cause any significant effect on the electronic state of the ferrocene moiety. This is in accordance with the chemical structure without conjugation between ferrocene and (cyclopentadiene)$Fe(CO)_3$ moieties. An anodic peak is observed at $E_{pa} = 0.9$ V, which can be attributed to irreversible oxidation of the (cyclopentadiene)$Fe(0)(CO)_3$ moiety, judging from the reported oxidation reaction of (η^4-diene)$Fe(CO)_3$-type complexes.[29]

The cyclic voltammogram of the mixtures of **2c** and **2a** given in Fig. 1b shows just two reversible waves at $E^{0\prime} = -0.06$ and 0.34 V, ascribed to the ferrocene moiety oxidation, in addition to an irreversible oxidation peak at $E_{pa} = 0.9$ V due to (cyclopentadiene)$Fe(CO)_3$. This also implies that the electronic effect of (cyclopentadiene)$Fe(CO)_3$ binding to ferrocene moieties is small, so that the redox potentials of **2c** are very close to those of **2a** ($E^{0\prime} = -0.07$ and 0.33 V) and **2b** ($E^{0\prime} = -0.10$ and 0.32 V).[5]

Similar consideration can be made for the cyclic voltammogram of a mixture of **3c** and **3a** in Fig. 1c, which displays three reversible oxidation waves at $E^{0\prime} = -0.10$, 0.12, and 0.51 V due to ferrocene moieties and an irreversible oxidation wave at $E_{pa} = 0.9$ V due to (cyclopentadiene)$Fe(CO)_3$ ($E^{0\prime}$'s of **3a** are −0.10, 0.12, and 0.51 V).[5] It should be noted that all the oxidation potentials of ferrocene moieties in **1c**, **2c**, and **3c** are more negative than those of (cyclopentadiene)$Fe(CO)_3$ moieties, ensuring that the changes in the electronic structure of ferrocene units in the whole redox process occur without oxidative decomposition of the (cyclopentadiene)$Fe(CO)_3$ moiety. This satisfies a condition requisite for the present IR spectroelectrochemical study to monitor the electronic structure of the ferrocene or oligoferrocenylene moiety by the change in the frequencies of CO stretching vibration for the iron tricarbonyl moiety.

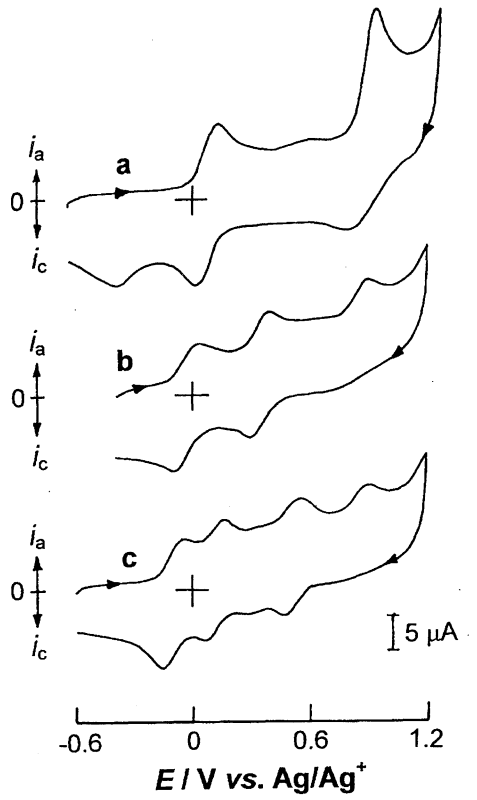

Fig. 1. Cyclic voltammetry of **1c** (a), **2c**+**2a** (b), and **3c**+**3a** (c) at GC in 0.1 mol dm^{-3} n-Bu_4NClO_4–CH_2Cl_2 at a scan rate of 0.1 V s^{-1}.

IR-Spectroelectrochemistry. Infrared spectroelectrochemistry was carried out using a Pt disk working electrode

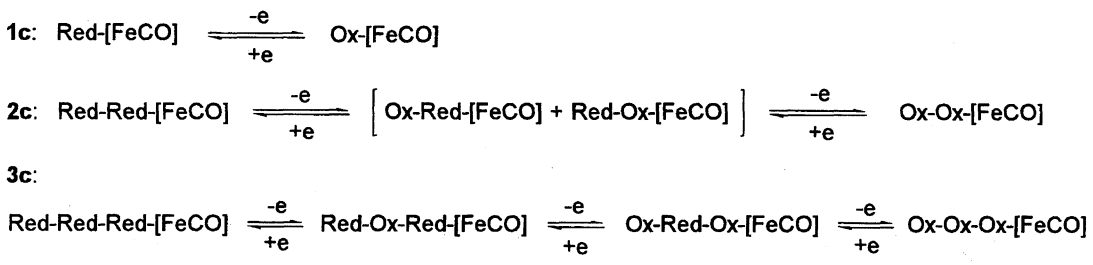

Scheme 2.

in a cell designed for IRAS measurements.[25] Cyclic voltammograms of **1c**, **2c**, and **3c** in this cell are similar to those at GC given in Fig. 1, except for large peak-to-peak separation (e.g., 180 mV for **1c**), because of the significant IR drop due to a thin solution layer on the working electrode. Infrared spectra of **1c** at given potentials in n-Bu_4NClO_4–CH_2Cl_2 are shown in Fig. 2, where the potentials allude to the spectra of reduced, oxidized and rereduced forms for a, b, and c, respectively. Both ν(CO) peaks shift to higher wavenumbers by 12 and 15 cm^{-1} by oxidation from $\mathbf{1c}^0$ to $\mathbf{1c}^+$ and the change is reversible. This direction of wavenumber shift is reasonable because the positively charged ferrocenium site withdraw electrons from Fe(II) in the (cyclopentadiene)Fe-$(CO)_3$ moiety, and consequently, back-donation from Fe to CO must be lessened. Wolf and Wrighton have reported a similar phenomenon: that the ν(CO) for a ruthenium carbonyl complex of poly(5,5′-di-2-thienyl-2,2′-bithiazole) shifts to higher energy by 4—6 cm^{-1} when the polythiophene backbone is oxidized.[30]

Figure 3 displays successive changes in the spectrum of **1c** with scanning the potential from 0 to 0.6 V vs. Ag/Ag^+. It is clearly seen that two sets of paired ν(CO) peaks appear in the potential range around $E^{0\prime}$ for the ferrocenium/ferrocene couple $\mathbf{1c}^+/\mathbf{1c}$, denying the possibility that the observed species is not a solute but an adsorbate and the wavenumber shift by the effect of electric field, because in such a case a gradual shift in wavenumbers should occur with the potential change. It can thus be concluded that the ν(CO) can sense the oxidation state of ferrocene unit bound to the (cyclopentadiene)$Fe(CO)_3$ moiety.

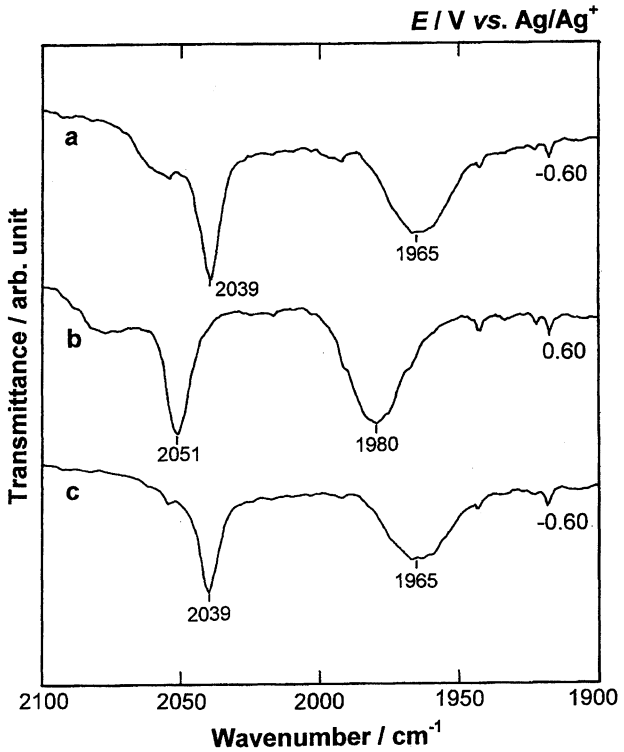

Fig. 2. IRAS spectra of **1c** at a Pt disk at given potentials in 0.1 mol dm^{-3} n-Bu_4NClO_4–CH_2Cl_2. The measurement was carried out in the alphabetic order.

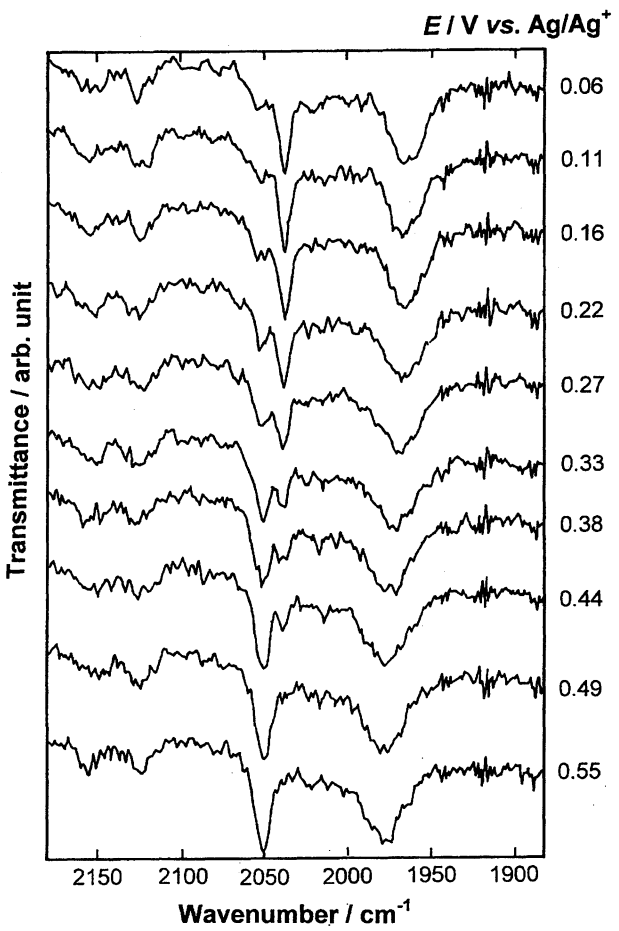

Fig. 3. IRAS spectra of **1c** obtained with scanning the potential from 0 to 0.6 V vs. Ag/Ag^+ in 0.1 mol dm^{-3} n-Bu_4NClO_4–CH_2Cl_2 at a scan rate of 0.1 V s^{-1}.

Infrared spectra of **2c** in three oxidation states are displayed in Fig. 4, showing a pair of peaks in each spectrum. The wavenumber shift for the pair from the fully reduced form at −0.60 V, $\mathbf{2c}^0$, to fully oxidized one at 0.62 V, $\mathbf{2c}^{2+}$, is 13 and 17 cm^{-1} in the higher direction and is reversible, similar to the case for the monomer, **1c**. In Fig. 4c, an extra broad peak appears around 2015 cm^{-1}. This peak can not be assigned to a signal of $\mathbf{2}^{2+}$ and its origin is unclear at this stage because of the difficulty in characterization of the species in electrolyte solution in the present experimental conditions. A possible candidate is a decomposition product of $\mathbf{2c}^{2+}$ because one can deduce that biferrocenium dication is less stable than biferrocene, judging from the facts that ferrocenium ion decomposes in a first order reaction in aqueous solution[31,32] and in a second order reaction in aprotic media.[33,34]

Two electronic isomers, Ox–Red–[FeCO] and Red–Ox–[FeCO] can exist in the mixed-valence state, $\mathbf{2c}^+$. If the electron-transfer rate between Red (Fe(II)) and Ox (Fe(III)) is slower than the time scale of IR, two sets of CO peaks should appear at wavenumbers similar to those of $\mathbf{2c}^0$ and $\mathbf{2c}^{2+}$. This is not the case in the spectrum of $\mathbf{2c}^+$, where a pair of peaks exist at the intermediate position between the

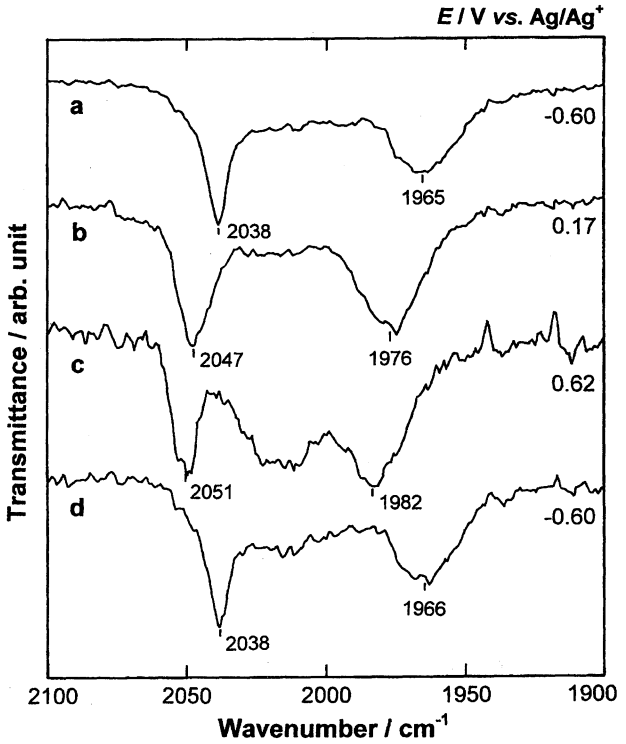

Fig. 4. IRAS spectra of **2c** (+**2a**) at a Pt disk at given potentials in 0.1 mol dm^{-3} *n*-Bu_4NClO_4–CH_2Cl_2. The measurement was carried out in the alphabetic order.

peaks for $\mathbf{2c}^0$ and $\mathbf{2c}^{2+}$. It has been reported that the KBr-pellet infrared spectra of mixed-valence cation of biferrocene and its derivatives hitherto known gives the absorption bands for perpendicular C–H bending mode attributable to both the Red (Fe(II)) and Ox (Fe(III)) parts of the mixed-valence ion at room temperature, indicating that the electron-transfer rates are less than ca. 10^{12} s^{-1}.[18—20] The difference in electron-transfer rate between these data and the present result should be due to a discrepancy in the condition of samples in the measurement; biferrocene is in solution in the present study but in KBr pellets in the previous studies. Reorganization of the matrix requisite for the thermal electron transfer is more restricted in the latter case, which makes the slower electron-transfer rate more significant.

Coexistence of both electronic isomers, Red–Ox–[FeCO] and Ox–Red–[FeCO], irrespective of the asymmetrical structure is probable because the electronic effect of (cyclopentadiene)$Fe(CO)_3$ is slightly different from that of H, as indicated by the similar redox potentials among **2a**, **2b**, and **2c** as mentioned above.

It should be noted that the peak width at half peak height of the 2047 cm^{-1} band (15 cm^{-1}) looks broader than that of **2c** and $\mathbf{2c}^{2+}$ (8 cm^{-1}), although the quality of the spectra is not sufficient to insist on this difference strenuously. Recently Ito et al. have reported the ν(CO) peak broadening in the mixed-valence pyrazine-bridged dimer of Ru trinuclear complex, indicating that the electron-transfer rate is comparable to the IR time scale, 10^{11}—10^{12} s^{-1}.[35] Thus, the result noted above may suggest a similar time-scale effect.

Infrared spectra for the trimer, **3c**, are shown in Fig. 5, showing reversible three-step changes for a pair of peaks, corresponding to formation of two mixed-valence states; the total wavenumber shifts from $\mathbf{3c}^0$ to $\mathbf{3c}^{3+}$ are 14 and 18 cm^{-1}, similar to those for the monomer and the dimer. Extra broad peaks observed around 2150 cm^{-1} in Figs. 5c, 5d, 5e, 5f, and 5g are probably due to a decomposition product of oxidized forms of **3c** (vide supra).

In case the electron transfer rate between Ox and Red in the mixed-valence states of the trimer, $\mathbf{3c}^+$ and $\mathbf{3c}^{2+}$ is faster than the IR time scale, and in case the thermodynamic stability is also the same for the three electronic isomers, Red–Ox–Red–[FeCO], Ox–Red–Red–[FeCO], and Red–Red–Ox–[FeCO] for $\mathbf{3c}^+$, Ox–Red–Ox–[FeCO], Ox–Ox–Red–[FeCO], and Red–Ox–Ox–[FeCO] for $\mathbf{3c}^{2+}$ so that the population of the isomers is same, the wave number shifts for the three oxidation steps should be one-third of the total shift, (14—18)/3 = 5—6 cm^{-1}. This is not consistent with the results shown in Fig. 5, where the most significant shifts, both 9 cm^{-1}, are observed at the second oxidation step.

The theory based on the neighboring site interaction indicates that Red–Ox–Red and Ox–Red–Ox are thermodynamically more favorable than Ox–Red–Red (=Red–Red–Ox) and Red–Ox–Ox (= Ox–Ox–Red), respectively, for the mixed-valence states of trimer.[7,8] This situation is entirely different from the dimer with two thermodynamically equivalent electronic isomers Red–Ox and Ox–Red in the mixed-valence state, as sketched in Fig. 6. Consequently, it can be

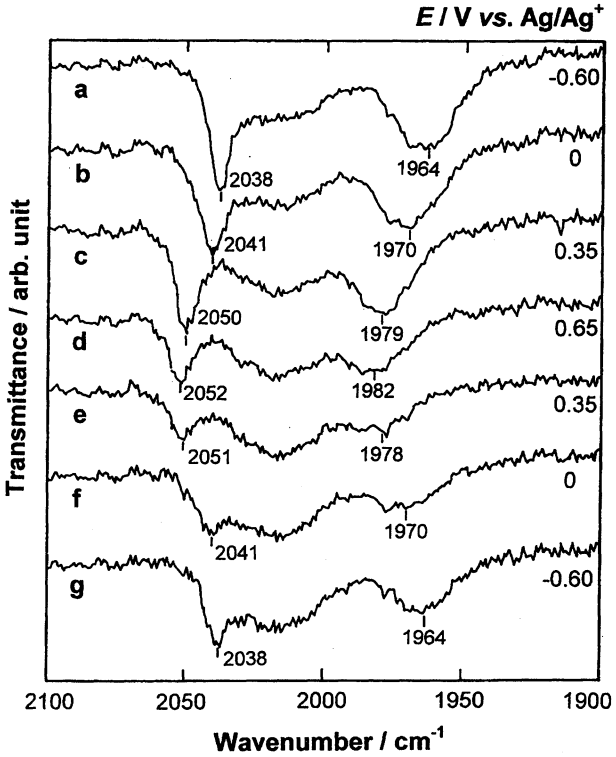

Fig. 5. IRAS spectra of **3c** (+**3a**) at a Pt disk at given potentials in 0.1 mol dm^{-3} *n*-Bu_4NClO_4–CH_2Cl_2. The measurement was carried out in the alphabetic order.

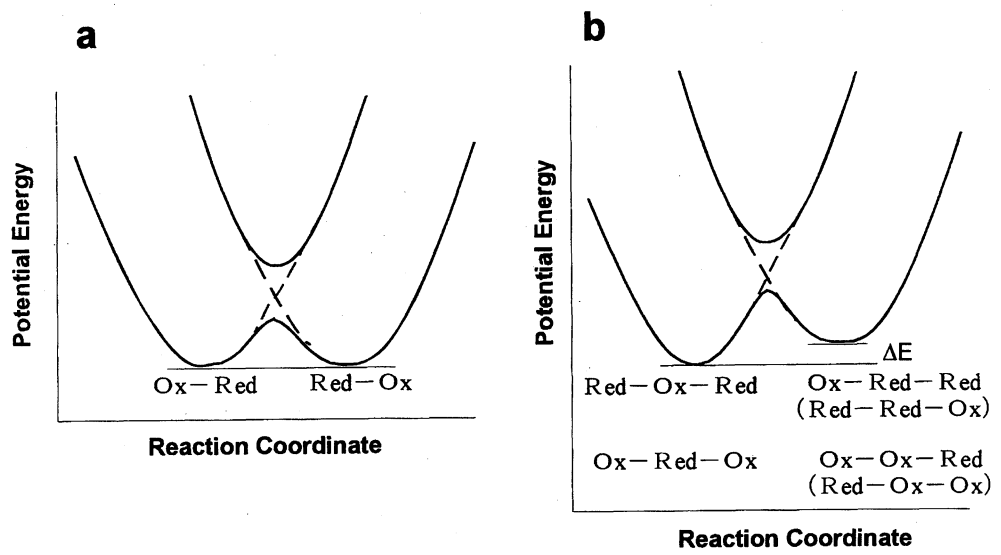

Fig. 6. Schematic illustration of the energy diagram on the mixed-valence states of biferrocene (a) and terferrocene (b).

expected for **3c** that the three-step oxidation pathway is composed of Red–Red–Red–Fe(CO)$_3$ ⟶ Red–Ox–Red–[FeCO] ⟶ Ox–Red–Ox–[FeCO] ⟶ Ox–Ox–Ox–[FeCO]; thus (cyclopentadiene)Fe(CO)$_3$-attached ferrocene site changes from Red to Ox at the second electron transfer step from monocation to dication. This prospect is roughly coincident with the largest wavenumber shift at the second oxidation step in Fig. 5.

One should recall that the IR result only indicates that the ferrocene site adjacent to (cyclopentadiene)Fe(CO)$_3$ is Red in monocation and Ox in dication, and thus Ox–Red–Red–[FeCO] and Red–Ox–Ox–[FeCO] can be the candidates as the forms of monocation and dication, respectively. This possibility can not be denied only by the spectral information, but the little difference in electronic effect between (cyclopentadiene)Fe(CO)$_3$ and H as noted above strongly supports the consideration that Red–Ox–Red–[FeCO] and Ox–Red–Ox–[FeCO] are thermodynamically more favorable than Ox–Red–Red–[FeCO] and Red–Ox–Ox–[FeCO], respectively.

Small wavenumber shifts are observed even at the first and third oxidation steps. As has been discussed above on **2c**, comparison of the IR time scale with the rate of electron transfer between Ox and Red in the mixed-valence states of **3c** is requisite primarily to elucidate the cause of these shifts, but the thermodynamic situation of electronic isomers in the mixed-valence states of **3c** is different from that of **2c** as illustrated in Fig. 6. The existence of an energy difference between the electronic isomers of $\mathbf{3c}^+$ and $\mathbf{3c}^{2+}$ indicates that the thermodynamically favorable Red–Ox–Red–[FeCO] of $\mathbf{3c}^+$ and Ox–Red–Ox–[FeCO] of $\mathbf{3c}^{2+}$ exist dominantly and transformation from Red–Ox–Red–[FeCO] to Ox–Red–Red–[FeCO] or Red–Red–Ox–[FeCO] for $\mathbf{3c}^+$, and that from Ox–Red–Ox–[FeCO] to Ox–Ox–Red–[FeCO] or Red–Ox–Ox–[FeCO] for $\mathbf{3c}^{2+}$ are much slower than that between the electronic isomers of $\mathbf{2c}^+$, Red–Ox–[FeCO] and Ox–Red–[FeCO] with no energy difference. This leads to a consideration that only Red–Ox–Red–[FeCO] and Ox–Red–Ox–[FeCO] should be observed in the IR spectra of $\mathbf{3c}^+$ and $\mathbf{3c}^{2+}$, respectively. This is supported by the result that only a pair of ν(CO) peaks appear for $\mathbf{3c}^+$ and $\mathbf{3c}^{2+}$, respectively, and these peaks are as sharp as those of $\mathbf{3c}^0$ and $\mathbf{3c}^{3+}$ in Fig. 5, while the peak of $\mathbf{2c}^+$ looks broader than $\mathbf{2c}^0$ and $\mathbf{2c}^+$ in Fig. 4 (vide supra).

Table 1. Data of ν_{CO} for (Cyclopentadiene)Fe(CO)$_3$-Bound Ferrocene Derivatives

Complex	Wavenumber/cm^{-1}		$\Delta\nu_{CO}$/cm^{-1}		$\Sigma\Delta\nu_{CO}/\Sigma\Delta\nu_{CO(total)}$
$\mathbf{1c}^0$	2039	1965	—	—	0
$\mathbf{1c}^{1+}$	2051	1980	12	15	1
$\mathbf{2c}^0$	2038	1965	—	—	0
$\mathbf{2c}^{1+}$	2047	1976	9	11	0.6—0.7
$\mathbf{2c}^{2+}$	2051	1982	4	6	1
$\mathbf{3c}^0$	2038	1964	—	—	0
$\mathbf{3c}^{1+}$	2041	1970	3	6	0.2—0.3
$\mathbf{3c}^{2+}$	2050	1979	9	9	0.8—0.9
$\mathbf{3c}^{3+}$	2052	1982	2	3	1

We assume at this stage that the wavenumber shifts in the first and third oxidation steps reflect partly the change in density on ferrocene sites binding to (cyclopentadiene)Fe(CO)$_3$, which should be caused by electron delocalization due to neighboring site interaction between Red and Ox. For example, the charge distribution in Red–Ox–Red is not (0)–(1)–(0) but (δ)–(1 − δ)–(δ) ($0 < \delta \ll 1$). It is simply evaluated that the shifts at the first and the third steps correspond to about 20 and 80% oxidation of the (cyclopentadiene)Fe(CO)$_3$-attached ferrocene site if the total wavenumber shift (14 and 18 cm^{-1}) corresponds to the full change in charge density of the ferrocene site from 0 to +1 and the shift in wavenumbers corresponds linearly to the change in charge (Table 1).

Conclusions

A pair of ν(CO) peaks appear in the infrared spectra of

1c, **2c**, and **3c** in CH_2Cl_2 and shift to higher wavenumbers (12—18 cm^{-1}) by the oxidation from the most reduced to the most oxidized forms due to a decrease in the degree of back-donation from Fe to CO. The ν(CO) peaks for the mixed-valence cation $\mathbf{2c}^+$ locate halfway between those for $\mathbf{2c}^0$ and $\mathbf{2c}^{2+}$, suggesting that the rate of internuclear electron-transfer is slower than or comparable to the time scale of infrared spectra (10^{11}—10^{12} s^{-1}). The terferrocene derivative **3c** shows ν(CO) frequency changes corresponding to the formation of two mixed-valence states. The shift is most significant at the step from $\mathbf{3c}^+$ to $\mathbf{3c}^{2+}$, supporting the consideration based on the neighboring site interaction that the oxidation process should be Red–Red–Red–[FeCO] ⟶ Red–Ox–Red–[FeCO] ⟶ Ox–Red–Ox–[FeCO] ⟶ Ox–Ox–Ox–[FeCO]. The partial wavenumber shifts in the first and third oxidation steps are attributed to modest charge delocalization in the mixed valence states.

This work was partly supported by Grants-in-Aid for Scientific Research (No. 09237101 on Priority Area Research of "Electrochemistry of Ordered Interfaces" and No. 09440226) from the Ministry of Education, Science, Sports and Culture, and by The Sumitomo Foundation. We thank Prof. K. Aoki at Fukui University for helpful discussions on the electrochemical behaviors, and Profs. M. Ito and Y. Shingaya at Keio University for IRAS measurements.

References

1) H. Nishihara, "Handbook of Organic Conductive Molecules and Polymers," et by H. S. Nalwa, Wiley, New York (1997), Vol. 2, Chap. 19, pp. 779—832, and the references therein.

2) E. W. Neuse, *J. Macromol. Sci.-Chem.*, **A16**, 3 (1981), and the references therein.

3) G. M. Brown, T. J. Meyer, D. O. Cowan, C. LeVanda, F. Kaufman, P. V. Roling, and M. D. Rausch, *Inorg. Chem.*, **14**, 506 (1975).

4) N. Oyama, Y. Takizawa, H. Matsuda, T. Yamamoto, and K. Sanechika, *Denki Kagaku*, **56**, 781 (1988).

5) T. Hirao, M. Kurashina, K. Aramaki, and H. Nishihara, *J. Chem. Soc., Dalton Trans.*, **1996**, 2929.

6) H. Nishihara, T. Hirao, K. Aramaki, and K. Aoki, *Synth. Met.*, **84**, 935 (1997).

7) K. Aoki and J. Chen, *J. Electroanal. Chem.*, **380**, 35 (1995).

8) K. Aoki, J. Chen, H. Nishihara, and T. Hirao, *J. Electroanal. Chem.*, **416**, 151 (1996).

9) In Ref. 7, analysis of redox potentials affords $u_1 = u_{OO} + u_{RR})/2 - u_{OR}$ and $u_2 = (u_{OO} - u_{RR})/2$ and u_{OX} is not determined rigorously. It can be, however, supposed that u_{OO} is positive because of coulombic repulsion and u_{RR} is neglectable so that u_{OR} is smaller than u_1, -15 kJ mol^{-1} and more than four times smaller than u_{OXR}, -3.8 kJ mol^{-1} (see Ref. 8).

10) D. O. Cowan, G. A. Candela, and F. Kaufman, *J. Am. Chem. Soc.*, **93**, 3889 (1971).

11) D. O. Cowan, R. L. Collins, and F. Kaufman, *J. Phys. Chem.*,**75**, 2025 (1971).

12) U. T. Mueller-Westerhoff and P. Elbracht, *J. Am. Chem. Soc.*, **94**, 9271 (1972).

13) F. Delgado-Pena, D. R. Talham, and D. O. Cowan, *J. Organomet. Chem.*, **253**, C43 (1983).

14) M. J. Cohn, T. Y.-Dong, D. N. Hendrickson, S. J. Geib, and A. L. Rheingold, *J. Chem. Soc., Chem. Commun.*, **1985**, 1095.

15) R. J. Wabb, P. M. Hagen, R. J. Wittebort, M. Sorai, and D. N. Hendrickson, *Inorg. Chem.*, **31**, 1791 (1992).

16) T.-Y. Dong, T.-Y. Lee, S.-H. Lee, G.-H. Lee, and S.-M. Peng, *Organometallics*, **13**, 2337 (1994).

17) .T.-Y. Dong, S.-H. Lee, C.-K. Chang, and K.-J. Lin, *J. Chem. Soc., Chem. Commun.*, **1995**, 2453.

18) W. H. Morrison and D. N. Hendrickson, *Inorg. Chem.*, **14**, 2331 (1975).

19) T.-Y. Dong, M.-J. Cohn, D. N. Hendrickson, and C. G. Pierpont, *J. Am. Chem. Soc.*, **107**, 4777 (1985).

20) T.-Y. Dong, D. N. Hendrickson, K. Iwai, M. J. Cohn, S. J. Geib, A. L. Rheingold, H. Sano, I. Motoyama, and S. Nakashima, *J. Am. Chem. Soc.*, **107**, 7996 (1985).

21) T.-Y. Dong, C.-H. Huang, C.-K. Chang, H.-C. Hsieh, S.-M. Peng, and G.-H. Lee, *Organometallics*, **14**, 1776 (1995).

22) J. A. Kramer and D. N. Hendrickson, *Inorg. Chem.*, **19**, 3330 (1980).

23) R. Rulkens, A. J. Lough, I. Manners, S. R. Lovelace, C. Grant, and W. E. Geiger, *J. Am. Chem. Soc.*, **118**, 12683 (1996).

24) E. H. Braye and W. Hübel, *Inorg. Synth.*, **8**, 178 (1966).

25) Y. Shingaya and M. Ito, *Surf. Sci.*, **368**, 318 (1996).

26) R. K. Kochhar and R. Pettit, *J. Organomet. Chem.*, **6**, 272 (1966).

27) M. A. Busch and R. J. Clark, *Inorg. Chem.*, **14**, 219 (1975).

28) G. Davidson, *Inorg. Chim. Acta*, **3**, 596 (1969).

29) N. G. Connelly, R. L. Kelly, M. D. Kitchen, R. M. Mills, F. D. Stansfield, M. W. Whiteley, S. M. Whiting, and P. Woodward, *J. Chem. Soc., Dalton Trans.*, **1981**, 1317.

30) M. O. Wolf and M. S. Wrighton, *Chem. Mater.*, **6**, 1526 (1994).

31) A. A. Pendin, M. S. Zakhar'evskii, and P. K. Leontevskaya, *Kinet. Katal.*, **7**, 1074 (1966).

32) R. Szentrimay, P. Yeh, and T. Kuwana, *ACS Symp. Ser.*, No. 38 (1977).

33) J. R. Lenhard and R. W. Murray, *J. Am. Chem. Soc.*, **100**, 7870 (1978).

34) H. Nishihara, M. Noguchi, and K. Aramaki, *Inorg. Chem.*, **26**, 2862 (1987).

35) T. Ito, T. Hamaguchi, H. Nagino, T. Yamaguchi, J. Washington, and C. P. Kubiak, *Science*, **277**, 660 (1997).